Analysis of Segmental Phosphate Absorption in Intact Rats

A Compartmental Analysis Approach

Laurie H. Kayne, David Z. D'Argenio, James H. Meyer, Ming Shu Hu, Nora Jamgotchian, and David B. N. Lee

Medical and Research Services, Veterans Affairs Medical Center, Sepulveda, California 91343; UCLA School of Medicine, Los Angeles, California 90024; and School of Engineering, University of Southern California, Los Angeles, California 90089

Abstract

Available information supports the dominance of the proximal intestine in inorganic phosphate (P_i) absorption. However, there is no strategy for analyzing segmental P_i absorption from a spontaneously propelled meal in an intact animal. We propose a solution using compartmental analysis. After intragastric administration of a ^{32}P-labeled P_i liquid meal containing a nonabsorbable marker, [^{14}C]polyethylene glycol (PEG), rats were killed at 2, 10, 20, 30, 60, 120, and 240 min. The gastrointestinal tract was removed and divided into seven segments, from which ^{32}P and [^{14}C]PEG were recovered. Data was expressed as a percentage of the dose fed, i.e., ($^{32}P_{[\text{in segment}]} \div {}^{32}P_{[\text{fed}]}$) and ([$^{14}C$]$PEG_{[\text{in segment}]} \div$ [^{14}C]$PEG_{[\text{fed}]}$), respectively. A compartmental model was constructed and the rate constants for intersegmental transit and segmental absorption were estimated. The "goodness of fit" between the simulated model and the actual data indicates the estimated rate constants reflect in vivo events. The duodenum, with the highest transit and absorption rates, accounted for a third of the total absorption. However, the terminal ileum, with a lower absorption rate but a longer transit time, absorbed an equal amount of P_i. This approach allows the analysis of the mechanism and the regulation of P_i absorption under more authentic in vivo conditions. (*J. Clin. Invest.* 1993. 91:915–922.) Key words: distal intestine • gastrointestinal transit • liquid meal • proximal intestine

Introduction

In previous studies in rat intestinal segments, we have demonstrated the presence of active inorganic phosphate (P_i) absorption in jejunum even in vitamin D–deficient (−D)[1] rats (1, 2). 1,25-Dihydroxyvitamin D (1,25D) repletion in these rats caused the induction of active P_i absorption in the duodenum and marked augmentation of active P_i absorption in the jejunum (1–3). Little or no active P_i absorption, in both −D and 1,25D-replete rats, was noted in the ileum (1) and the colon (4). These and similar findings by others (5) have led to the consensus that the bulk of P_i absorption is accomplished in the proximal intestine (6). However, all of these studies were based on measurements in isolated intestinal segments, bathed in or perfused with artificial solutions. The segmental contribution to P_i absorption in a living animal, however, can only be assessed in an intestine in which the natural physiological conditions and regulatory mechanisms are not altered and the forward progression of the meal is not impeded.

Although many studies have evaluated total intestinal P_i absorption in vivo (5, 7), only three have attempted to resolve this total P_i absorption into components contributed by different intestinal segments. In one study in the rat, the transit rate was measured in one group of animals and the absorptive rate for P_i was measured in ligated intestinal loops in a different group of animals (8). The failure to measure transit and absorption simultaneously in the same animal and the disruption of the anatomical and physiological continuity of the intestine cast doubt on the observations as truly reflecting in vivo events. In the other two studies in chicks (9) and laying hens (10), respectively, absorption was measured at only one time point, and the relationship of this time point to the meal was not clearly defined. These constraints raise difficulties in interpreting the data because P_i absorption in a given segment would be expected to vary with time after the administration of a meal.

In the current study we propose a new approach to the analysis of in vivo segmental P_i absorption. A compartmental model describing the transit and absorption of P_i was developed from the experimental data. This model was then used to estimate the rate of P_i absorption and the percentage of P_i absorbed by the different intestinal segments over time. The "goodness of fit" found between the experimental data and the curves generated by the simulated model suggests that compartmental analysis can be applied to the in vivo analysis of segmental P_i (or other nutrients) absorption from a food bolus advancing unhindered through the gastrointestinal tract.

Methods

Study design. 43 male Sprague-Dawley rats weighing 100–150 g and fed a diet that contained 1.2% and 0.8% of Ca and P_i, respectively, were used for all experiments. The liquid meal (0.85 ± 0.04 ml) was given by gastric gavage (5Fr, 15-in. Pharmaseal tubing, Baxter Healthcare Corp., Valencia, CA) after an 18-h fast. Rats were fed between 10 and 11 a.m. each day in all experiments. After administration of the feeding solution the animals were deprived of food and water. Rats were anesthetized by intraperitoneal injection of sodium pentobarbital (50 mg/kg) at 2 (n = 4), 10 (n = 9), 20 (n = 7), 30 (n = 6), 60 (n = 8), 120 (n = 5), and 240 (n = 3) min after intragastric feeding. The number of rats used at each time point was determined by the variability of the observations at that time point. Immediately after anesthesia the abdomen was opened and the gastrointestinal tract exposed. The gastrointestinal tract was immediately clamped at the esophageal–gastric junction

This work was presented in part at the 1992 FASEB Meeting, Anaheim, CA, 5–9 April 1992.

Address reprint requests to Dr. Lee, Nephrology Section (111R), Veterans Affairs Medical Center, 16111 Plummer Street, Sepulveda, CA 91343-2036.

Received for publication 19 May 1992 and in revised form 8 September 1992.

1. *Abbreviations used in this paper:* AUC, area under the curve; 1,25D, 1,25-dihydroxyvitamin D; −D, vitamin D–deficient (rats); MRT, mean residence time.

and above the anus. As shown in Fig. 1, the entire intestine was then removed and divided into seven segments: stomach, the duodenum (10 cm), four equal segments of the remaining small intestine (20–24 cm each—proximal segment 1, proximal segment 2, distal segment 1, and distal segment 2), and cecum/colon. The length of the small intestine for all the rats was 99±5 cm.

Although there is general agreement on the duodenum as the segment that extends from the pylorus to the ligament of Treitz, there is less consensus on the definition for the jejunum or the ileum. This is because there is not a distinct anatomical site that separates the two segments. In the human, the jejunum is generally defined as the first two-fifths of the intestine past the ligament of Treitz and the ileum as the last three-fifths of the small intestine (11). In the rat, however, the term "ileum" has been used to refer to only the last 10 cm (as in Ussing studies [12]) to as much as the entire second half of the small intestine past the ligament of Treitz in whole-animal studies (8). As a generalization, our proximal segments 1 and 2 would represent the conventionally defined jejunum, and our distal segments 1 and 2, the ileum.

Each segment was perfused with 35 ml of normal saline (0.9% NaCl). The amount of saline perfused was based on a previous report in the literature (13) and also on the amount determined in our laboratory to effectively remove the entire dose of [^{14}C]polyethel glycol [^{14}C]-PEG. The perfusate was weighed and samples were analyzed for ^{32}P and [^{14}C]PEG.

Placement of the feeding tube. To determine the length required for intragastric feeding, three rats were anesthetized and dissected to expose the esophagus and stomach, and feeding tubes were advanced through the mouth into the stomach of each rat (14). A length of 9 cm was required to position the tip of the feeding tube in the stomach of all three rats. The position of the feeding tube was further confirmed by filling a feeding tube with 1 ml of barium sulfate and advancing the tube 9 cm in a fasted and anesthetized rat. X-ray films were taken before and after injection of 1 ml of barium sulfate. The pictures revealed the tip of the tube was in the fundus and the injected contrast was found only in the stomach.

Liquid meal. A liquid meal not containing other nutrients was used to allow comparison with other studies measuring mineral absorption (8, 15, 16). The liquid meal contained sodium phosphate (10 mg/ml), PEG (mol wt 4,000, 1 g/100 ml), 2 μCi ^{14}C-labeled PEG ([^{14}C]PEG, 60 mci/mmol), and 1 μCi ^{32}P tracer (9,000 Ci/mmol). ^{32}P and [^{14}C]-PEG were used as markers of P_i and PEG movement. PEG served as a nonabsorbable, liquid-phase marker (17, 18) to document movement of the meal through the intestinal tract and as a reference against which P_i absorption was measured.

The concentration of P_i used in the present study was based on previous studies conducted in rats (8, 15, 19) and humans (20). Studies have used concentrations that ranged from 0, i.e., tracer only (8, 15) to 240 mM (20). In the present study we decided to use a concentration of 83 mM. At this concentration we were giving the rats 2.19 mg P.

Radioisotope analysis. To determine ^{32}P and [^{14}C]PEG activity in samples, aliquots were taken and counted in duplicate in a two-channel liquid scintillation counter (model LS 5801, Beckman Instruments, Inc., Palo Alto, CA) that automatically corrected for quench and spillover.

Calculations. In each rat, total recovery of [^{14}C]PEG and ^{32}P was determined by summing the activities recovered in all individual segments. The total intestinal P_i absorption (in percent dose) was calculated as $[1 - (^{32}P/[^{14}C]PEG)_{\text{from all segments}} \div (^{32}P/[^{14}C]PEG)_{\text{from feed}}] \times 100$. The segmental recoveries of PEG and P_i at any time point were expressed as a percentage of the amount fed and were calculated as $([^{14}C]PEG_{[\text{in segment}]} \div [^{14}C]PEG_{[\text{fed}]})$ and $(^{32}P_{[\text{in segment}]} \div {}^{32}P_{[\text{fed}]})$, respectively.

The mean residence time of PEG, rate of P_i absorption, and percent P_i absorbed by each segment were estimated using compartmental analysis. The compartmental model shown in Fig. 2 was used for this purpose and represents transit and absorption of P_i assuming first-order kinetics. Fig. 1 summarizes the definitions of the seven intestinal segments, which are represented by the larger boxes in Fig. 2. The model shown in Fig. 2 depicts compartments as smaller boxes, transit rate constants as $k_{21}, k_{32}, \ldots k_{87}$ (k_{ij} represents transit from j to i), and absorption rate constants as $k_{02}, k_{03}, \ldots k_{07}$ (k_{0i} represents absorption from i. No detectable P_i absorption occurred from the stomach (compartment 1). Because of the significant transit delays occurring in the last three segments (distal segments 1 and 2, and cecum/colon), as evident from inspection of the segmental P_i and PEG data, it was not reasonable to model these segments as single homogeneous compartments. Instead, each of these segments was represented by a series of identical compartments with the same transit (k_{65}, k_{76}, or k_{87}) and absorption (k_{05}, k_{06}, or k_{07}) rate constants. The numbering of the rate constants in distal segments 1 and 2 and cecum/colon reflects this assumption and refers to segment and not compartment numbers. The total number of compartments selected to represent each of these three segments was determined by a "goodness of fit" analysis of simulated models (see below). Administration of the liquid meal was modeled as a bolus injection into the stomach, compartment 1 in Fig. 2. The six shaded compartments (16 through 21), correspond to output from compartments 2, 3, and 4, the sum of the output from compartments 5 through 8, the sum of the output from compartments 9 through 13, and the sum of the output from compartments 14 and 15.

Compartment model rate constants were estimated using the nonlinear, ordinary least squares estimation capabilities of the ADAPT II pharmacokinetic modeling package (21). To estimate all the rate constants of the model shown in Fig. 2, the following two-step procedure was used. First, the compartment model was used to estimate seven PEG transit rate constants ($k_{21}, k_{32}, k_{43}, k_{54}, k_{65}, k_{76}, k_{87}$), assuming no PEG absorption (i.e., $k_{02} = k_{03} = k_{04} = k_{05} = k_{06} = k_{07} = 0.0$). Next the P_i data were used to estimate the six absorption rate constants, with the transit rate constants fixed at their least squares estimates obtained from the PEG data. This is based on the assumption that P_i and PEG transit through the gastrointestinal tract at the same rate. Based on the movement of the markers observed in this study, this assumption appeared valid (see results). Approximate values for the standard deviations of all rate constant estimates were also obtained (see Landow and DiStephano [22]). In order to arrive at the model shown in Fig. 2, the above two-step estimation procedure was implemented using candidate models with different numbers of compartments to represent distal segments 1 and 2 and cecum/colon. Adding more compartments than shown in Fig. 2 to represent the delays in these distal segments

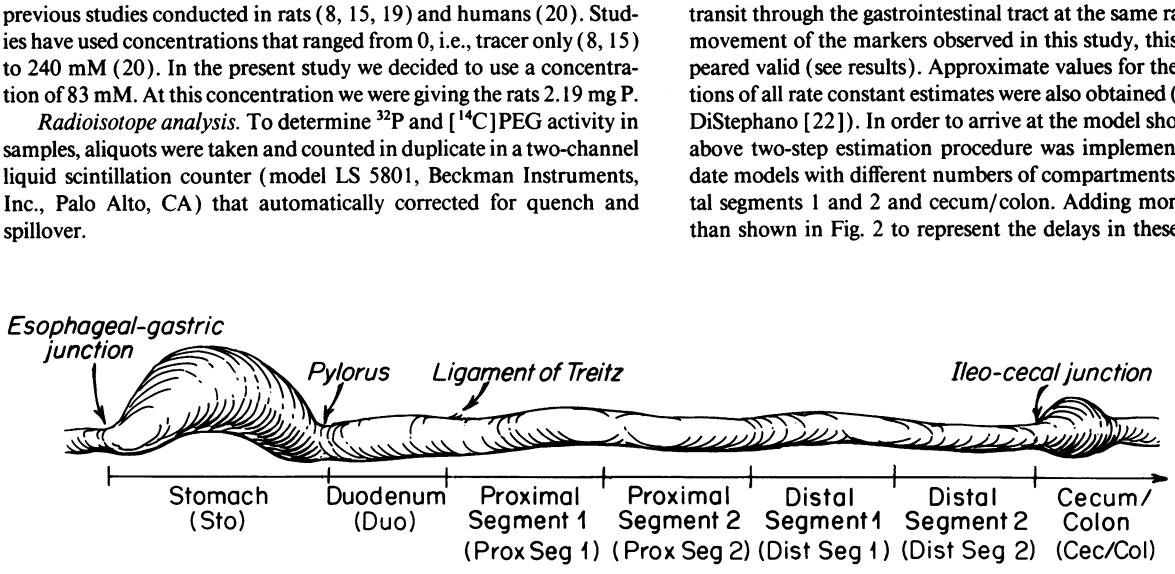

Figure 1. Definition of intestinal segments.

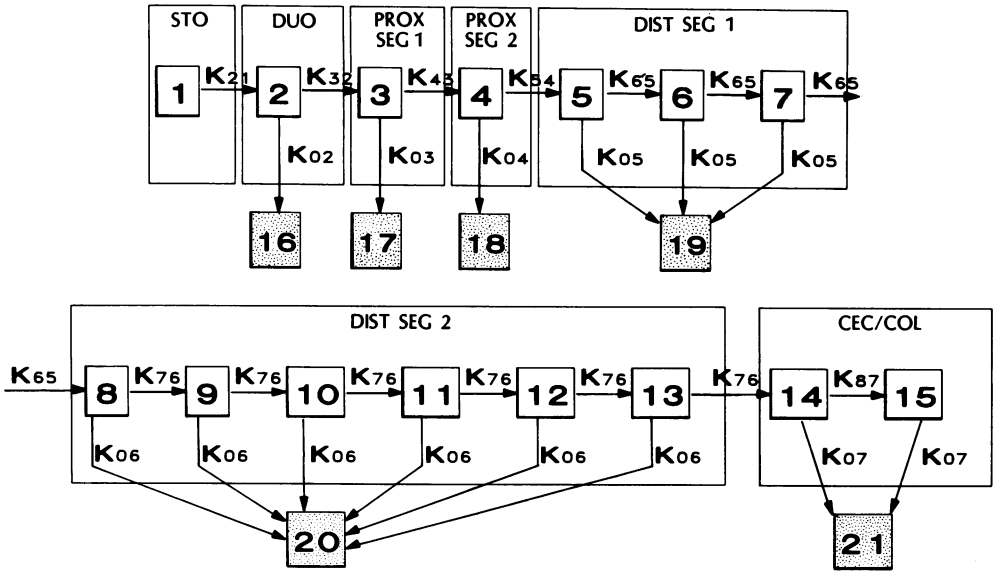

Figure 2. Diagram of 21-compartment model representing the gastrointestinal tract. The intestinal segments sto, duo, prox seg 1, and prox seg 2 are represented by compartments 1 through 4, respectively. Dist seg 1 is represented by compartments 5–7. Dist seg 2 is represented by compartments 8–13, and the cec/col is represented by compartments 14 and 15. k_{21}, k_{32}, k_{43}, k_{54}, k_{65}, k_{76}, and k_{87} are the transit rate constants for each intestinal segment. k_{02}, k_{03}, k_{04}, k_{05}, k_{06}, and k_{07} are the absorption rate constants. Compartments 16 through 21 represent the percentage of P_i absorbed by the intestinal segments was estimated by the percentage of P_i in compartments 16 through 21 using the estimated rate constants. Definitions of the segments and corresponding abbreviations are shown in Fig. 1.

produced < 1% reduction in the overall sum of squares. It should be noted that all the measured data for each of the segments was used to define the least squares criterion for the PEG and P_i data. In both cases a total of 272 observations were used (32 for stomach, 36 for duodenum, 36 for proximal segment 1, 42 for proximal segment 2, 42 for distal segment 1, 42 for distal segment 2, and 42 for cecum/colon).

Using the least squares estimates of the rate constants, the compartment model of Fig. 2 was simulated to predict the percent P_i absorbed by duodenum, proximal segment 1, proximal segment 2, distal segment 1, and distal segment 2 (no absorption was reliably detected in cecum/colon, see below). These were estimated as the activities in compartments 16 through 21 at 10, 20, 30, 60, 120, and 240 min after administration of the liquid meal. The associated standard deviations for percent P_i absorbed by each segment were estimated with the Monte Carlo simulation option (n = 500) of ADAPT II (21), using the least squares estimates for the rate constants and their standard deviations to define a log-normal distribution for each parameter. Absorption rate profiles, i.e., the rate of P_i absorbed from the duodenum through the terminal ileum as a function of time, denoted as $\text{rabs}_{\text{duo}}(t)$, . . . , $\text{rabs}_{\text{dist seg 2}}(t)$, were constructed from the model as follows [($x_i(t)$ represents the simulated P_i activity in the ith compartment]: $\text{rabs}_{\text{duo}}(t) = k_{02}x_2(t)$; $\text{rabs}_{\text{prox seg 1}}(t) = k_{03}x_3(t)$; $\text{rabs}_{\text{prox seg 2}}(t) = k_{04}x_4(t)$; $\text{rabs}_{\text{dist seg 1}}(t) = k_{05}[x_5(t) + x_6(t) + x_7(t)]$; $\text{rabs}_{\text{dist seg 2}}(t) = k_{06}[x_8(t) + x_9(t) + x_{10}(t) + x_{11}(t) + x_{12}(t) + x_{13}(t)]$. Finally, the mean residence time (MRT) of PEG in each segment (MRT_{sto} through $\text{MRT}_{\text{dist seg 2}}$) were calculated from the least squares estimates of the transit rate constants as follows: $\text{MRT}_{\text{sto}} = 1/k_{21}$; $\text{MRT}_{\text{duo}} = 1/k_{32}$; $\text{MRT}_{\text{prox seg 1}} = 1/k_{43}$; $\text{MRT}_{\text{prox seg 2}} = 1/k_{54}$; $\text{MRT}_{\text{dist seg 1}} = 3/k_{65}$; $\text{MRT}_{\text{dist seg 2}} = 6/k_{76}$.

Values are presented as means±SD, except where noted in the text.

Results

Recovery of P_i and PEG. Total recovery of PEG was 89±6%. Recovery of P_i was 90% at 2 min and then progressively decreased with time due to absorption.

Intestinal transit of PEG and P_i. The movement of PEG through the intestine over time is shown in Fig. 3. At 20 min ~ 80% of the recovered PEG was at or beyond proximal segment 2 and by 2 h virtually all of the recovered PEG had reached distal segment 2. An identical transit pattern was observed for P_i (not shown), suggesting that the two solutes advanced through the gastrointestinal tract at the same rate.

The least squares estimates for the transit rate constants obtained by fitting the compartment model (Fig. 2) to the collected PEG data are listed in Table I. The standard deviation obtained for k_{87} was > 10 times higher than the estimate and therefore was not included in the analysis. The PEG activities predicted by this fitted model are shown in Fig. 3 along with the measured data (shown as mean±SD) for each of the seven measured segments (all of the data were used in the parameter estimation). The correlation coefficient (r) for the seven segments, stomach, duodenum, proximal segment 1, proximal segment 2, distal segment 1, distal segment 2, and cecum/colon, are 0.99, 0.81, 0.87, 0.80, 0.82, 0.93, and 0.98, respectively. The estimates of the MRT for PEG in each segment are as follows: stomach, 5.6±0.03 min; duodenum, 2.7±0.3 min; proximal segment 1, 5.8±0.5 min; proximal segment 2, 29.8±2.6 min; distal segment 1, 51.1±3.5 min; distal segment 2, 106.4±11.7 min. These results indicate that transit through the stomach, duodenum, and proximal segment 1 are comparable, whereas there is a progressive reduction in the rates of transit through the more distal segments.

P_i absorption. Absorption of P_i from the liquid meal over time is shown in Fig. 4. About 40% of the P_i fed was absorbed in the first 30 min and 91% was absorbed by 2 h.

Table II gives the least squares estimates for the absorption rate constants along with their standard deviations for each intestinal segment. The standard deviation for the estimate of k_{07} was > 10 times higher than the estimated value suggesting the absence of absorption in cecum/colon in this study. Fig. 5 shows the model predictions for the percent P_i in each segment along with the measured data shown as the mean±SD. The r values for the stomach, duodenum, proximal segment 1, proximal segment 2, distal segment 1, distal segment 2, and cecum/

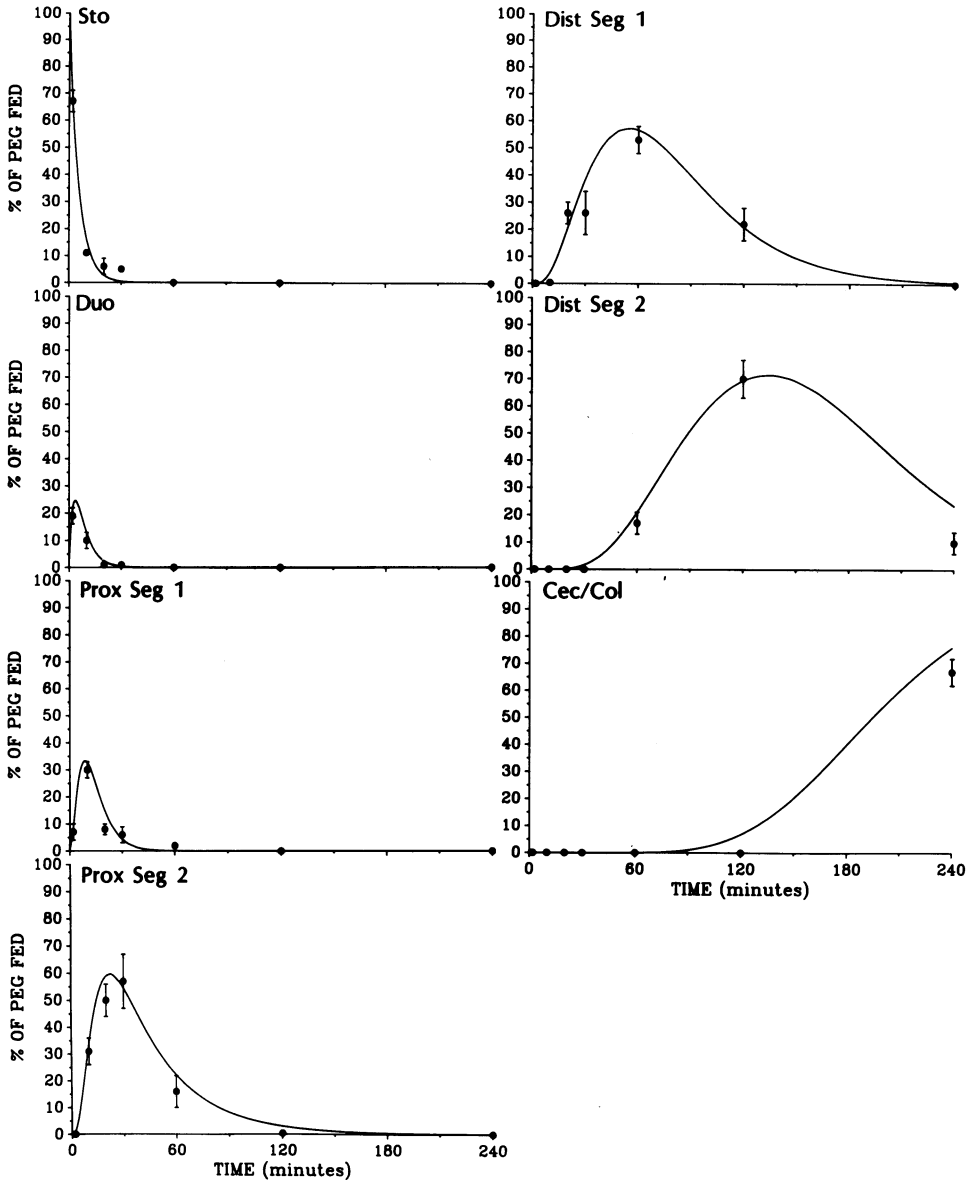

Figure 3. Fitting of the compartmental model to the PEG data. For each segment, the means (•)±SD for the observed data are shown. The solid line shows the percentage PEG over time that is predicted from the estimated transit rate constants in the compartmental model. Estimation of the transit rate constants is described in Table I. A total of 272 observations were used.

colon are 0.97, 0.90, 0.87, 0.82, 0.78, 0.74, 0.81, and 0.90, respectively. The estimated P_i absorption rate profiles for the small intestine segments (see Methods) are displayed in Fig. 6. Inspection of these curves indicates that the maximal rate of P_i absorption is substantially higher in the duodenum than in any other segment.

Table III shows the estimated values of percent P_i absorbed (±SD) by the small intestine segments at five of the observation time points. The duodenum and distal segment 2 (terminal ileum) each absorbed one-third of the total P_i dose with the remaining one-third absorbed by the rest of the intestine in between.

Discussion

In the current study we have developed a model for analyzing segmental solute P_i absorption from a spontaneously propelled liquid meal in vivo. As discussed earlier, of the few studies published, none has satisfied the theoretical and experimental considerations associated with absorption from a continuously moving food bolus through an untampered gastrointestinal tract (8–10).

A more rigorous study design was used by Marcus and Lengemann in analyzing segmental calcium absorption in vivo (16, 23). Animals fed either a liquid or a solid diet containing ^{47}Ca and a nonabsorbable isotopic marker, ^{91}Y were killed in incremental time intervals after feeding. Based on the recovery of these isotopes in consecutive intestinal segments, a ^{47}Ca curve and a ^{91}Y curve were generated for each segment defining the amount of each isotope remaining in the segment over time. The area under the curve (AUC) for ^{47}Ca was then subtracted from the AUC for ^{91}Y for each segment and this difference in AUC was taken to represent the Ca absorption which had occurred up to a given segment. Based on such calculations, they concluded that the bulk of in vivo Ca absorption occurred in ileum. ^{91}Y and ^{47}Ca, however, did not move through the gastrointestinal tract at the same rate (16, 23). In addition, Fig. 7 attempts to examine the validity of equating the difference in AUCs to the absorption of Ca. Schematized ^{47}Ca and ^{91}Y curves are depicted in a proximal segment with a

Table I. Estimates of Transit Rate Constants

Parameter	Estimate
	min^{-1}
k_{21}	0.180±0.009
k_{32}	0.373±0.040
k_{43}	0.172±0.015
k_{54}	0.034±0.003
k_{65}	0.059±0.004
k_{76}	0.056±0.006

Values are estimates of the transit rate constants±SD. The estimates are based on data from 100–150-g fasted rats (n = 42) after intragastric feeding of a liquid meal containing [^{14}C]PEG, 10 mg of PEG, ^{32}P, and 10 mg of sodium phosphate. At various time points rats were killed and the intestine was removed. The segments were perfused with saline and the perfusate counted for [^{14}C]PEG and ^{32}P. The percent PEG in each segment was determined for each rat. Estimates for k_{21}, k_{32}, k_{43}, k_{54}, k_{65}, and k_{76} were obtained by fitting the compartmental model (Fig. 1) with the absorption rate constants set at zero to the PEG data using the nonlinear least squares estimation procedure contained in ADAPT II (21). The associated covariance matrix was also calculated to determine the SD for each transit rate constant. See Fig. 2 for definitions of parameters.

Table II. Estimates of P_i Absorption Rate Constants

Parameter	Estimate
	min^{-1}
k_{02}	0.198±0.060
k_{03}	0.015±0.027
k_{04}	0.017±0.008
k_{05}	0.004±0.006
k_{06}	0.035±0.010

Values are estimates±SD of the P_i absorption rate constants in the intestine based on data from 100–150-g fasted rats (n = 42) after intragastric feeding of a liquid meal containing [^{14}C]PEG, 10 mg of PEG, ^{32}P, and 10 mg of sodium phosphate. At various time points rats were killed and the intestine was removed. The segments were perfused with saline and the perfusate counted for [^{14}C]PEG and ^{32}P. The percent dose P_i in each segment was determined for each rat. The absorption rate constants k_{02}, k_{03}, k_{04}, k_{05}, k_{06}, and k_{07} were estimated by fitting the compartmental model (Fig. 2) to the P_i data using the nonlinear least squares estimation procedure contained in ADAPT II (21). The transit rate constants were set at values obtained in Table I. The associated covariance matrix was also calculated to determine the SDs for each absorption rate constant. See Fig. 2 for definitions of parameters.

rapid transit time (10 min, *left panel*) and a subsequent segment with a slower transit time (120 min, *right panel*). The ratio of AUC^{47}Ca to AUC^{91}Y was 2:3 in the early segment, suggesting that one-third of the Ca in the meal had been absorbed up to this segment (assuming the ratio of the absorbable Ca to the nonabsorbable ^{91}Y was 1 in the meal). This ratio remained unchanged in the subsequent segment indicating no further extraction of Ca has occurred. However, from the difference in AUCs (^{91}Y – ^{47}Ca), represented respectively, by α_1 and α_2, one would conclude that Ca absorption in the more distal segment was greater, in that α_2 was clearly greater than α_1. Thus, calculation of absorption based on difference in AUCs would erroneously attribute greater absorption to the segment with the longer transit time.

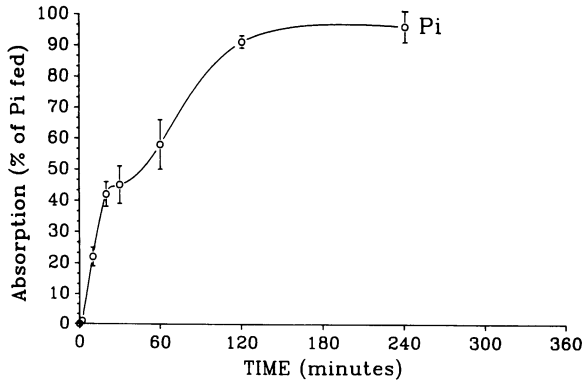

Figure 4. Absorption of P_i as a function of time after intragastric administration of ^{32}P and [^{14}C]PEG to fasting Sprague-Dawley rats (100–150 g). See Table I for methods. Percentage of fed P_i absorbed was calculated from the equation: 1-[(^{32}P/[^{14}C]PEG recovered from the rat)/(^{32}P/[^{14}C]PEG fed)]. Data are expressed as means±SE, n = 3–9.

We propose an approach using compartmental analysis, a technique frequently employed in pharmacokinetic studies. This form of analysis has been used to describe the dynamic disappearance rates of a drug from the circulation following its administration into different "compartments." We have adapted this principle to analyze the in vivo, dynamic absorption rate (disappearance rate) of a solute (drug) from the intestinal lumen (circulation) of different segments after the intragastric administration of a liquid meal.

The compartment model developed from the experimental data assumes that the fluxes of ^{32}P and [^{14}C]PEG are governed by first-order kinetics, are in the directions indicated by the arrows in Fig. 2, and that the distribution of ^{32}P and [^{14}C]PEG within each compartment is homogeneous. Because PEG is not absorbed, it is a reasonable approximation to consider its fluxes are governed by first-order kinetics. For P_i, given the level fed (83 mM), the passive process is dominant and can be described by first-order kinetics (7). Cramer (8) has previously demonstrated negligible secretion into the gastrointestinal tract of administered ^{32}P 6 h after the dose. His study, therefore, indicates that the second assumption is valid. In order to account for the significant delays occurring in distal segments 1 and 2, and cecum/colon, each of these segments was modeled by a series of identical compartments (with the same transit and absorption rate constants). This approach satisfies the third assumption and seems reasonable in that we are only interested in the overall transit and absorption properties of these segments, and not in the kinetic inhomogeneities that may exist along the length of each of the segments. Given these assumptions, the model allows for the estimation in each segment of the mean residence time of the meal, the rate of P_i absorption, and percent P_i absorbed (Tables I–III). The plausibility of the model is supported by its ability to describe the experimental data (Figs. 3 and 5), and suggests that the model can be used to provide estimates of in vivo P_i transport and absorption kinetics in different intestinal segments.

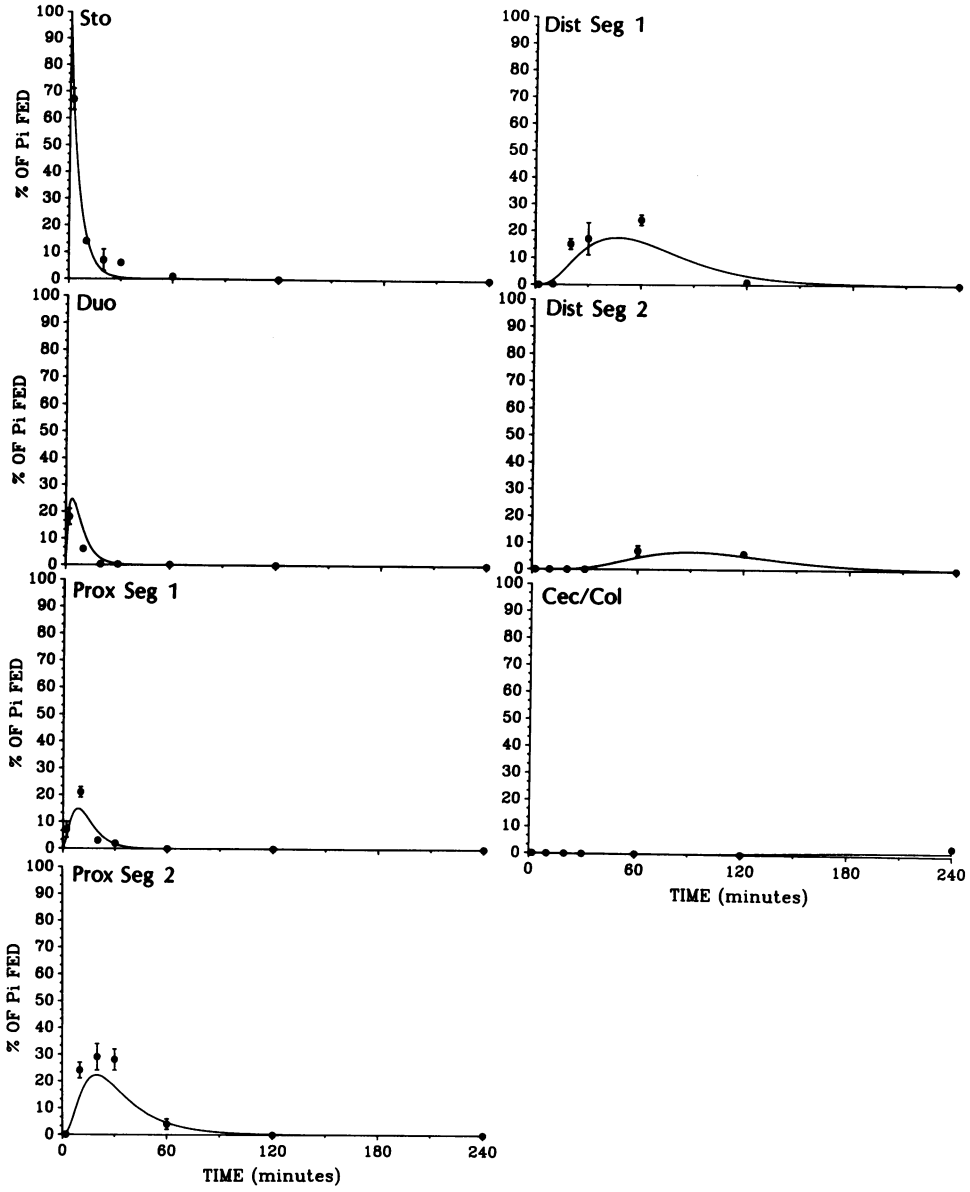

Figure 5. Fitting of the compartmental model to the P_i data. For each segment, the means (●)±SD for the observed P_i data are shown. The solid line shows the percent P_i over time that is predicted from the estimated transit and P_i absorption rate constants in the compartmental model. Estimation of the rate constants is described in Tables I and II. Definitions of segments are shown in Fig. 1. A total of 272 observations were used.

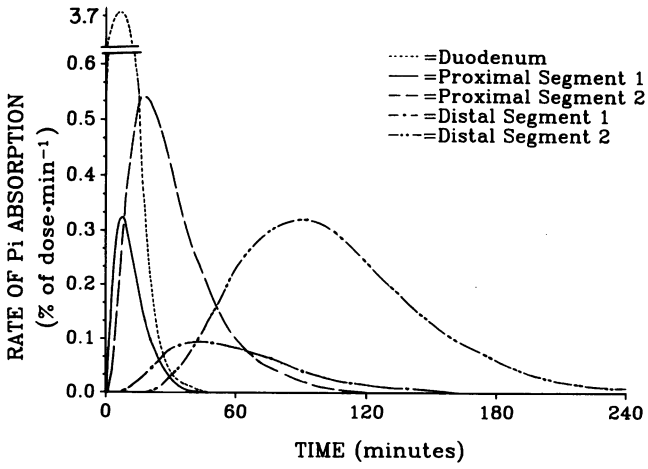

Figure 6. Segmental P_i absorption rate profiles. The P_i absorption rates for each segment are shown over time. The rates of P_i absorbed from the duodenum through distal segment 2 as a function of time were constructed from the compartmental model (see Methods).

Consistent with previous reports (8, 24, 25), we observed rapid gastric emptying of the liquid meal and rapid movement through the proximal small intestine. 90% of the administered meal left the stomach by 10 min. As early as 10–20 min after administration, the meal began to appear in the distal small intestine and almost all of the recovered dose reached the terminal ileum (distal segment 2) by 2 h. The transit rate of the meal, however, slowed dramatically as the meal moved down the intestine. The mean residence time of the liquid meal went from 6 min in the duodenum to 52 min in distal segment 1 and 116 min in the distal segment 2. Traditionally, the early appearance of an orally administered isotopic P_i in blood has been interpreted to reflect the contribution of absorption by the proximal intestine (5, 25). Our data, however, demonstrate that a liquid meal arrives in the distal small intestine as early as 10–20 min after its consumption. This raises the possibility that the early appearance of an enterally administered nutrient in the circulation may derive from the distal intestine as well.

Our choice of using a liquid meal (8, 16) and the P_i concentration (8, 19, 20) is based on the majority of published studies

Table III. Segmental P_i Absorption over Time

Segment	Time				
	10	30	60	120	240
			min		
Duodenum	26±5	34±7	34±7	34±7	34±7
Proximal segment 1	2±3	4±5	4±5	4±5	4±5
Proximal segment 2	1±0.7	11±4	18±6	19±7	20±7
Distal segment 1	0	0.9±1	3±4	6±6	6±7
Distal segment 2	0	0.2±0.1	4±1	22±6	33±9

Values represent the percentage P_i absorption occurring in each intestinal segment in 100–150-g fasted rats fed a liquid dose of P_i and PEG. The percentage P_i absorbed by each segment was estimated via Monte Carlo simulation of the estimated compartment model. The transit rate constants and the absorption rate constants were set at the values obtained in Tables I and II. Each parameter estimate and its standard deviation were used to define the log-normal parameter distributions that were incorporated into the Monte Carlo simulation (see Methods).

on the measurement of total P_i absorption from an experimental meal. The high percentage absorption (96%) may be attributed to the relatively small quantity of P_i fed after an overnight fast and the use of young growing rats. P_i absorption began within the first 10 min after feeding and was completed by 2 h (Fig. 4).

P_i absorption rate constant was highest in the duodenum, which exhibited a value 50 times greater than the lowest rate constant measured in distal segment 1 (Table II). Fig. 6, however, also illustrates that while the duodenum has the highest maximal rate of absorption, the rapid movement of the meal through this segment quickly lowered absorption to zero and limited total P_i absorption in the duodenum to only 34% of the dose (Table III). In contrast, distal segment 2 (terminal ileum), despite having a much lower absorption rate constant (Table II), continued absorbing P_i over a substantially longer period of time (Fig. 6) due to the slower movement of the liquid meal (Table I). The result was that distal segment 2 ended up absorbing as much P_i (33%, Table III) as the duodenum. The remaining one-third of the absorbed P_i was accomplished in the intervening small intestine with proximal segment 2 playing the major role (20%, Table II). Thus, the contribution to total P_i absorption was fairly evenly distributed between duodenum (35%), jejunum (25%, proximal segments 1 and 2), and ileum (40%, distal segments 1 and 2).

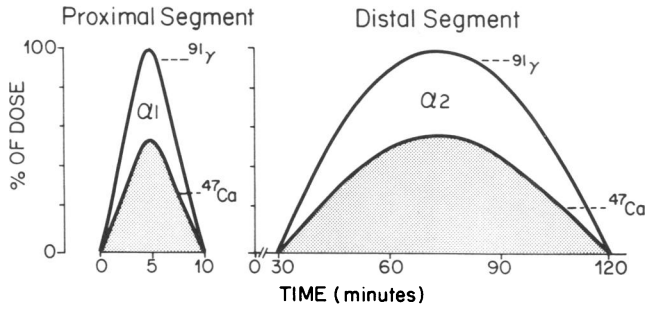

Figure 7. Representative curves of ^{91}Y and ^{47}Ca in proximal and distal intestinal segments over time. $\alpha 1$ and $\alpha 2$ represent the difference areas obtained by subtracting the AUC of ^{47}Ca from the AUC of ^{91}Y. $\alpha 2$ is substantially larger than $\alpha 1$, suggesting that absorption of ^{47}Ca was highest in the distal segment. The ratios of AUC ^{47}Ca to AUC ^{91}Y in both the proximal and distal segment, however, are the same (2:3), indicating that in fact no further absorption has occurred in the distal segment.

These observations highlight the limitations of studies using isolated intestinal segments in predicting the physiology of P_i absorption in an untampered intestinal tract. Our results suggest that in the intact intestine, the distal small intestine which is poorly adapted for P_i absorption when studied in isolation (7), absorbs as much P_i as the more proximal segments endowed with highly efficient P_i absorptive mechanism(s). The longer mean residence time in the distal small intestine which translates into longer contact time for absorption is an important factor. In addition, it is possible that local luminal factors may increase the availability of P_i for absorption and/or activate additional transport mechanisms for P_i absorption, e.g., the presence of bile salts in the distal intestine in vivo can increase P_i transport through the intercellular pathway (27).

It should be pointed out that despite the differences in methodology used, our data are surprisingly similar to those of Cramer (8). Cramer reported that 38% of the P_i administered was absorbed in the ileum which he defined as the distal 42 cm. In our study the ileum (distal segments 1 and 2) representing the distal 40–45 cm absorbed 40% of the P_i dose. In addition, Cramer's data also indicated substantial absorption in the proximal small intestine. The first 12 cm distal to the pylorus (equivalent to our duodenum) accounted for 29% and the middle 42 cm (proximal segments 1 and 2 in our study) accounted for 25% of total P_i absorption.

In conclusion, we have demonstrated that the technique of compartmental modeling can be used to analyze and integrate segmental absorptive events of P_i from a spontaneously propelled liquid meal along the intact intestinal tract of normal conscious rats. This opens up the exciting opportunity of reexamining many of the important mechanistic and regulatory mechanisms, established (virtually without exception) from experimental models that have been anatomically or physiologically altered. In our model, animals were anesthetized not to obtain postmortem events, but to obtain "snap-shot" information on premortem events, generated under completely untampered conditions. This new technique is also potentially applicable to the in vivo analysis of segmental absorption of other nutrients.

Acknowledgments

The authors gratefully acknowledge Dr. Ron Navarro for taking the X-rays, Mark Hori for numerous technical discussions, Dr. Janet Elashoff for statistical consultation, Sashi Reddy for excellent technical assistance, and Dr. Paul Sternberg's laboratory at the California Institute of Technology for the use of computer facilities.

This study was supported in part by Department of Veterans Affairs Medical Research Support and by National Institutes of Health grant P43-RR01861. Dr. Laurie H. Kayne was a Research Fellow of the National Kidney Foundation of Southern California and of the American Heart Association Greater Los Angeles Affiliate.

References

1. Walling, M. R. 1977. Intestinal Ca and phosphate transport: differential responses to vitamin D_3 metabolites. *Am. J. Physiol.* 233:E488–E494.

2. Lee, D. B. N., M. W. Walling, and N. Brautbar. 1986. Intestinal phosphate absorption: Influence of vitamin D and non-vitamin D factors. *Am. J. Physiol.* 250:G369–G373.

3. Lee, D. B. N., M. W. Walling, and D. B. Corry. 1986. Phosphate transport across rat jejunum: influence of sodium, pH, and 1,25-dihydroxyvitamin D_3. *Am. J. Physiol.* 251:G90–G95.

4. Lee, D. B. N., M. W. Walling, V. Silis, U. Gafter, and J. W. Coburn. 1980. Calcium and inorganic phosphate transport in rat colon. Dissociated response to 1,25-dihydroxyvitamin D_3. *J. Clin. Invest.* 65:1326–1331.

5. Nordin, B. E. C. 1976. Calcium, Phosphate, and Magnesium Metabolism. Churchill Livingstone, London. 96–112.

6. Peterlik, M. 1985. Intestinal phosphate transport. *In* The Enzymes of Biological Membranes, Volume 3. A. N. Martonisi, editor. Plenum Press, New York. 287–320.

7. McHardy, G. J. R., and D. S. Parsons. 1956. The absorption of inorganic phosphate from the small intestine of the rat. *Q. J. Exp. Physiol.* 41:398–409.

8. Cramer, C. F. 1961. Progress and rate of absorption of radiophosphorus through the intestinal tract of rats. *Can. J. Biochem. Physiol.* 39:499–503.

9. Hurwitz, S., and A. Bar. 1970. The sites of calcium and phosphate absorption in the chick. *Poultry Sci.* 49:324–325.

10. Hurwitz, S., and A. Bar. 1965. Absorption of calcium and phosphorus along the gastrointestinal tract of the laying fowl as influenced by dietary calcium and effective shell formation. *J. Nutr.* 86:433–438.

11. Haubrich, W. S. 1985. Gross anatomy of the small intestine. *In* Bockus Gastroenterology, Volume 3, Fourth edition. J. E. Berk, editor. W. B. Saunders Co., Philadelphia. 1474–1478.

12. Nellans, H. N., and D. V. Kimberg. 1979. Anomalous calcium secretion in rat ileum: role of paracellular pathway. *Am. J. Physiol.* 236:E473–E481.

13. Wasserman, R. H., and A. N. Taylor. 1973. Intestinal absorption of phosphate in the chick: effect of vitamin D and other parameters. *J. Nutr.* 103:586–599.

14. Gershon-Cohen, J., and H. Shay. 1962. Gastrointestinal examination of rat. *In* The Rat in Laboratory Investigation. E. J. Farris, and J. Q. Griffith, editors. Hafner, New York. 426–433.

15. Cramer, C. F. 1959. In vivo measurement of radiophosphorus and radiostrontium absorption in rats. *PSEBM (Proc. Soc. Exp. Biol. Med.)* 100:364–367.

16. Marcus, C. S., and F. W. Lengemann. 1962. Absorption of Ca45 and Sr85 from solid and liquid food at various levels of alimentary tract of the rat. *J. Nutr.* 77:155–160.

17. Meyer, J. H., E. A. Meyer, D. Jehn, Y. G. Gu, A. D. Fink, and M. Fried. 1986. Gastric processing and emptying of fat. *Gastroenterology.* 90:1176–1187.

18. Miller, D. L., H. P. Schedl, J. Bouska, and S. F. Phillips. 1987. Food restriction and recovery of nonabsorbed indicators from the small intestine of the rat. *Digestion.* 38:83–89.

19. Nicolaysen, R. 1937. Studies upon the mode of action of vitamin D. V The absorption of phosphates from isolated loops of the small intestine in the rat. *Biochem. J.* 31:1086–1088.

20. Condon, J. R., J. R. Nassim, and A. Rutter. 1970. Defective intestinal phosphate absorption in familial and non-familial hypophosphataemia. *Br. Med. J.* 3:138–141.

21. D'Argenio, D. Z., and A. Schumitzky. 1990. Adapt Users Guide. Biomedical Simulations Resource, University of Southern California, Los Angeles.

22. Landow, L. M., and J. J. DiStefano. 1984. Multiexponential, multicompartmental and noncompartmental modeling. II. Data analysis and statistical considerations. *Am. J. Physiol.* 246:R665–677.

23. Marcus, C. S., and F. W. Lengemann. 1962. Use of radioyttrium to study food movement in the small intestine of the rat. *J. Nutr.* 76:179–182.

24. Poulakos, L., and T. H. Kent. 1973. Gastric emptying and small intestinal propulsion in fed and fasted rats. *Gastroenterology.* 64:962–967.

25. Malagelada, J. R., J. S. Robertson, J. L. Brown, M. Remington, J. A. Duenes, G. M. Thomforde, and P. W. Carryer. 1984. Intestinal transit of solid and liquid components of a meal in health. *Gastroenterology.* 87:1255–1263.

26. Caniggia, A., C. Gennari, M. Bencini, and V. Polazzouli. 1968. Intestinal absorption of radiophosphate. *Calcif. Tissue Res.* 2:299–300.

27. Freel, R. W., M. Hatch, D. L. Earnest, and A. M. Goldner. 1983. Role of tight-junctional pathways in bile salt-induced increases in colonic permeability. *Am. J. Physiol.* 245:G816–G823.